ISSN 2394-3777 (Print)
ISSN 2394-3785 (Online)
Available online at www.ijartet.com
International Journal of Advanced Research Trends in Engineering and Technology (IJARTET)
Vol. 4, Issue 3, March 2017

SEGMENTATION OF DEFOCUS BLUR BASED ON LLBP

D.Samatha (M.Tech.) [1]

Mrs.K.Vani (Asst.Professor) [2]

Dr. B. Hari Krishna (Professor,PhD) [3]

Mr.C.Ashok Kumar (Professor) [4]

[1,2,3,4] CMR Engineering College, Kandlakoya, Hyderabad, T.S, (501401), INDIA

samatha.dayal@gmail.com[1] vanireddycp@gmail.com[2] harikrishna07@gmail.com[3]

cdkumarecehod.cmrecl@gmail.com[4]

Abstract---Defocus obscure is to a great degree basic in pictures caught utilizing optical imaging frameworks. It might be unwanted, however may likewise be a purposeful aesthetic impact, accordingly it can either upgrade or restrain our visual view of the picture scene. For errands, for example, picture rebuilding and question acknowledgment, one might need to fragment an incompletely obscured picture into obscured and non-obscured districts. In this paper, we propose sharpness metric in light of nearby twofold examples and a strong division calculation to isolate all through concentration picture locales. The proposed sharpness metric endeavors the perception that most nearby picture fixes in foggy areas have essentially less of certain neighborhood parallel examples contrasted and those in sharp districts. Utilizing this metric together with picture tangling and multiscale surmising, we got great sharpness maps. Tests on several somewhat obscured pictures were utilized to assess our obscure division calculation and six comparator strategies. The outcomes demonstrate that our calculation accomplishes similar division comes about with the best in class and have huge speed advantage over the others.

List of Terms: Defocus, obscure, division, LBP, nearby double examples, picture reclamation, question acknowledgment, out-of-center, obscured,LLBP.

I. INTRODUCTION

In advanced picture catching, obscure frequently shows up in a picture. Obscure sorts in the pictures incorporate out-of-center and movement obscure, where out-of-center obscure is caused by the arrangement of a question out of camera profundity of field, and movement obscure is because of movement of the camera or the protest. In both obscure sorts, fractional obscure shows up when a piece of the picture is obscured. There are a few applications for fractional obscure discovery and division, for example, halfway deblurring, quality evaluation and picture criminology.

Picture division is the way toward apportioning a computerized picture into numerous areas. The objective of division is to disentangle or potentially change the portrayal of a picture into something that is more vital and simpler to look at. Picture division is commonly used to find questions and foundation in pictures. All the more precisely, picture division is the way toward allotting a name to each pixel in a picture to such an extent that pixels with a similar mark share certain visual qualities. Picture division is an imperative flag handling instrument that is generally utilized in numerous applications including object discovery, protest based coding, question following, picture recovery, and clinical organ or tissue distinguishing proof. Thresholding is the essential strategy for picture division. Shape a grayscale picture, can be utilized to create double

ISSN 2394-3777 (Print)
ISSN 2394-3785 (Online)
Available online at www.ijartet.com
International Journal of Advanced Research Trends in Engineering and Technology (IJARTET)
Vol. 4, Issue 3, March 2017

pictures. The possibility of this technique is to choose the edge esteem.

Visual saliency is the perceptual quality that makes a question, individual, or pixel emerge in respect to its neighbors and along these lines catch our consideration. Visual consideration comes about both from quick, pre-mindful, base up visual saliency of the retinal contribution, and additionally from slower, top-down memory and volition based handling that is errand subordinate [24]. The concentration of this paper is the programmed identification of outwardly striking districts in pictures, which is valuable in applications, for example, versatile substance conveyance [22], versatile area of-intrigue based picture pressure [4], picture division [18, 9], question acknowledgment [26], and content mindful picture resizing [2]. Our calculation discovers low-level, pre-mindful, base up saliency. It is enlivened by the natural idea of focus encompass differentiate, however did not depend on any organic model.

Current techniques for saliency location produce areas that have low determination, ineffectively characterized fringes, or are costly to process. Also, a few techniques create higher saliency esteems at protest edges as opposed to producing maps that consistently cover the entire question, which comes about because of neglecting to abuse all the spatial recurrence substance of the first picture. We investigate the spatial frequencies in the first picture that are held by five best in class strategies, and outwardly delineate that these procedures principally work utilizing to a great degree low-recurrence content in the picture. We acquaint a recurrence tuned approach with appraise focus encompass differentiate utilizing shading and luminance includes that offers three favorable circumstances over existing strategies: consistently featured remarkable locales with all around characterized limits, full determination, and computational proficiency. The saliency delineate can be all the more successfully utilized as a part of numerous applications, and here we exhibit comes about for question division. We give a target examination of the precision of the saliency maps against five best in class strategies utilizing a ground truth of a 1000 pictures. Our strategy beats these strategies as far as exactness and review.

2. LITERATURE SURVEY

Fergus et al. [1] proposed a method that Camera shakes during exposure May causes to objectionable image blur and damage photographs. Conventional blind deconvolution techniques rarely assume frequency-domain parameters on images for the motion path while camera shake. Real camera motions can follow up the convoluted way and spatial domain prior can better retains visually image properties. They introduced a method to remove the effects of camera shake from blurred images. This method assumes that a uniform camera blur over the image and also negligible in-plane camera rotation. In order to calculate the blur from the camera shake, the person must specify an image region without saturation effects. They showed results for a wide variety of digital photographs which are taken from personal photo collections.

Bae and Durand[2] presented the image processing technique in which defocus magnification is used to perform blur estimation. To maximize defocus blur caused by lens aperture by taking a single image then estimate the size of blur kernel at edges and further they spread this technique to the whole image. In this approach multi scale edge detector is used and model fitting that obtain the size of bur propagate the blur measure by assuming that blurriness is smooth where intensity and color are approximately similar. Using defocus map, they enhance the existing blurriness, which means that blur the blurry regions and keeps the sharp regions sharp. In comparison to other methods more difficult issues arises such as depth from defocus, so this proposed method do not need precise depth estimation and do not need to disambiguate texture less regions. The method models changes in energy at all frequencies with blur and not just very high frequencies (edges).

Levin et al. [3] evaluate Blind deconvolution algorithm which is the restoration of a sharp version from a blurred image when the blur kernel is not

ISSN 2394-3777 (Print)
ISSN 2394-3785 (Online)
Available online at www.ijartet.com
International Journal of Advanced Research Trends in Engineering and Technology (IJARTET)
Vol. 4, Issue 3, March 2017

known. Most algorithms have dramatic progress; still many aspects of the problem remain challenging and difficult to understand. The goal of this method is to analyze and evaluate blind deconvolution algorithms both theoretically as well as experimentally. They had also discussed the failure of the MAP approach.

Kee et al. [4], discussed that noticeable blur is generated due to the optical system of the camera, also with professional lenses. They introduce method to measure the blur kernel densely over the image and also across multiple aperture and zoom settings. It shown that the blur kernel can have a non-negligible spread, even with top-of-the-line equipment. the spatial changes are not gradually symmetric and not even left-right symmetric .In this method two models of the optical blur are developed and compared both having advantages respectively. It is shown that the model find accurate blur kernels that can be used to restore images. They demonstrated that they can produce images that are more uniformly sharp then those images which produced with spatially-invariant deblurring technique.

Tai and brown in [5] As Image defocus estimation is useful for several applications including deblurring, blur enlargement, measuring image quality, and depth of field segmentation. They proposed a simple effective approach for estimating a defocus blur map based on the relationship of the contrast to the image gradient in a local image region and call this relationship the local contrast prior. The advantage of this approach is that it does not need filter banks or frequency decomposition of the input image; infact it only needs to compare local gradient profiles with the local contrast. They discuss the idea behind the local contrast prior and shown its results on a variety of experiments. And it"s found that for natural in-focus images, this distribution follows a similar pattern. They verified this distribution by plotting the distribution of the LC in images suffered from different type of degradation. This prior is useful in estimating defocus blur, in segmenting in focus regions from depth-of-field image and in ranking image quality. [9] discussed about a system, GSM based AMR has low infrastructure cost and it reduces man power. The system is fully automatic, hence the probability of error is reduced. The data is highly secured and it not only solve the problem of traditional meter reading system but also provides additional features such as power disconnection, reconnection and the concept of power management. The database stores the current month and also all the previous month data for the future use. Hence the system saves a lot amount of time and energy. Due to the power fluctuations, there might be a damage in the home appliances. Hence to avoid such damages and to protect the appliances, the voltage controlling method can be implemented.

3. PROPOSED METHOD

Local Binary Patterns (LBP) have been successful for computer vision problems such as texture segmentation, face recognition, background subtraction and recognition of 3D textured surfaces [36]. The LBP code of a pixel (xc,yc)is defined as

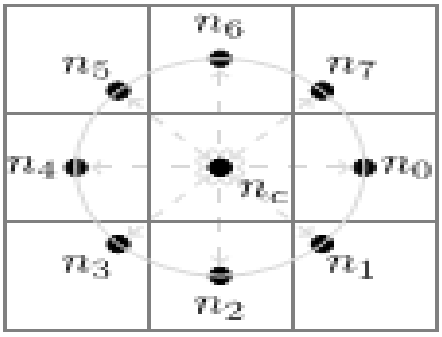

Fig. 1. 8-bit LBP with p=8,R=1

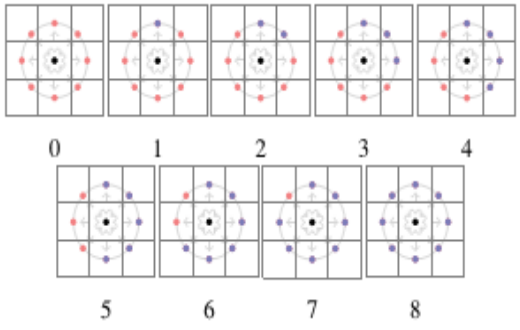

Fig. 2. The uniform rotationally invariant LBP.

ISSN 2394-3777 (Print)
ISSN 2394-3785 (Online)
Available online at www.ijartet.com
International Journal of Advanced Research Trends in Engineering and Technology (IJARTET)
Vol. 4, Issue 3, March 2017

$$LBP_{P,R}(x_c, y_c) = \sum_{p=0}^{P-1} S(n_p - n_c) \times 2^P$$

$$\text{With } S(x) = \begin{cases} 1 & |x| \geq T_{LBP} \\ 0 & |x| < T_{LBP} \end{cases} \qquad (3.1)$$

Where c is the intensity of the central pixel (x_c, y_c), n_p corresponds to the intensities of the P neighboring pixels located on a circle of radius R centered at n_c, and TLBP>0 is a small, positive threshold in order to achieve robustness for flat image regions as in [19]. Figure 4 shows the locations of the neighboring pixels n_p for P=8 and R=1. In general, the point's n_p do not fall in the center of image pixels, so the intensity of n_p is obtained with bilinear interpolation. A rotation invariant version of LBP can be achieved by performing the circular bitwise right shift that minimizes the value of the LBP code when it is interpreted as a binary number.

In this way, number of unique patterns are reduced to 36. Ojala et al. found that not all rotation invariant patterns sustain rotation equally well [34], and so proposed using only uniform patterns which are a subset of the rotation invariant patterns. A pattern is uniform if the circular sequence of bits contains no more than two transitions from one to zero, or zero to one. The non-uniform patterns are then all treated as one single pattern. This further reduces the number of unique patterns to 10 (for 8-bit LBP), that is, 9 uniform patterns, and the category of non-uniform patterns. The uniform patterns are shown in Figure 5. In this figure, neighboring pixels are colored blue if their intensity difference from centre pixel is larger than TLBP, and we say that it has been "triggered", otherwise, the neighbours are colored red.

Our proposed sharpness metric exploits these observations:

$$m_{LBP} = \frac{1}{N} \sum_{i=6}^{9} n\left(LBP_{8,1}^{riu2} i\right) \qquad (3.2)$$

Where $n\left(LBP_{8,1}^{riu2} i\right)$is the number of rotation invariant uniform 8-bit LBP pattern of type i,and N is the total number of pixels in the selected local region which serves to normalize the metric so that m_{LBP}∈[0,1]. One of the advantages of measuring sharpness in the LBP domain is that LBP features are robust to monotonic illumination changes which occur frequently in natural images. The threshold TLBP in Equation (3.1) controls the proposed metric's sensitivity to sharpness.

There is a sharp fall-off between σ =0.2 and σ=1.0 which makes the intersection of response value range of sharp and blur much smaller than the other metrics. When σ approaches 2, responses for all patches shrinks to zero which facilitates segmentation of blurred and sharp regions by simple thresholding. Moreover, almost smooth region elicit a much higher response than smooth region compared with the other metrics. Finally, the metric response is nearly monotonic, decreasing with increasing blur, which should allow such regions to be distinguished with greater accuracy and consistency.

LLBP segmentation operation :

LDP and LBP are utilized to extricate the double codes from the improved pictures. Despite the fact that the execution of LDP is superior to the LBP, the calculation time for LDP is around 2.5 times slower than the LBP. In addition, the code length for LDP is four times longer than the LBP. The calculation time and format estimate are two vital variables that should be considered in outlining a biometric framework. To beat the previously mentioned issues, the double codes in this work are extricated from the upgraded pictures utilizing another surface descriptor called Local Line Binary Pattern (LLBP) . One of the advantages of LLBP administrator is that it can underline the adjustment in picture power, for example, vertices, edges and corners.

Propelled by LBP, Petpon and Srisuk proposed a LLBP administrator for confront acknowledgment. The administrator comprises of two segments: level segment and vertical segment. The extent of LLBP can be acquired by computing the line double codes for the two segments. The delineation of LLBP administrator is appeared in Figure 6, and its mathematic definitions are given in Equations (4)–(6). LLBPh, LLBPv and LLBPm are LLBP on even course, vertical heading, and its greatness, separately.

ISSN 2394-3777 (Print)
ISSN 2394-3785 (Online)
Available online at www.ijartet.com
International Journal of Advanced Research Trends in Engineering and Technology (IJARTET)
Vol. 4, Issue 3, March 2017

N is the length of the line in pixel, hn is the pixel alongside the even line and vn is the pixel alongside the vertical line, c=N2 is the position of the inside pixel hc on the level line and vc on the vertical line, and s(•) work characterizes a thresholding capacity as in Equation (3).

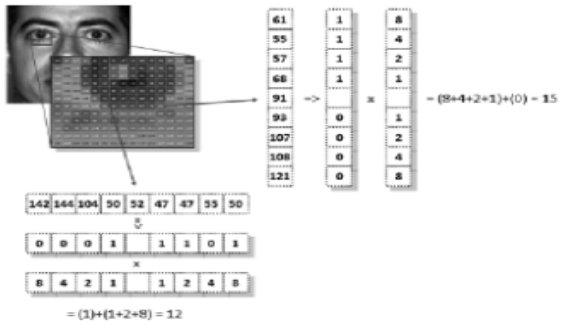

Fig.3.LLBP operator with line length 9 pixels, 8 bits considered

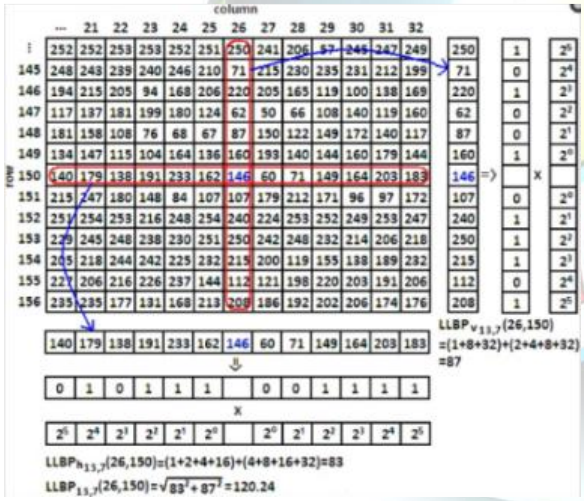

Fig.4. Example of LLBP operator

$$s(x) = \begin{cases} 1, & x \geq 0, \\ 0, & x < 0. \end{cases} \tag{3}$$

$$LLBP_{hN,c}(x,y) = \sum_{n=1}^{c-1} s(h_n - h_c) \cdot 2^{c-n-1} + \sum_{n=c+1}^{N} s(h_n - h_c) \cdot 2^{n-c-1} \tag{4}$$

$$LLBP_{vN,c}(x,y) = \sum_{n=1}^{c-1} s(v_n - v_c) \cdot 2^{c-n-1} + \sum_{n=c+1}^{N} s(v_n - v_c) \cdot 2^{n-c-1} \tag{5}$$

$$LLBP_m = \sqrt{LLBP_h^2 + LLBP_v^2} \tag{6}$$

Extraction of hearty highlights from finger vein pictures is a vital issue in a finger vein based biometric framework. Rather than utilizing LBP and LDP, we propose to utilize the nearby line twofold example (LLBP) as highlight extraction method. The straight-line state of LLBP can extricate hearty highlights from the pictures with misty veins. Test comes about on the pictures from 204 fingers that are caught from our own particular model gadget demonstrate that the equivalent mistake rate (EER) for the LLBP is essentially lower than the LBP and LDP. In addition, the component extraction time for LLBP is quicker than the other LBP variations. We additionally discover that the vertical segment of LLBP is the most appropriate for finger vein acknowledgment. In future, we intend to intertwine the highlights from the finger vein pictures with the state of a finger utilizing different combination methods. We trust that the EER can be additionally lessened by the combination of these two highlights.

NEW BLUR SEGMENTATION ALGORITHM

This section presents our algorithm for segmenting blurred/sharp regions with our LBP-based sharpness metric it is summarized in Figure 12. The algorithm has four main steps: multi-scale sharpness map generation, alpha matting initialization, alpha map computation, and multi-scale sharpness inference.

A. Multi-Scale Sharpness Map Generation

In the first step, multi-scale sharpness maps are generated using m_{LBP}. The sharpness metric is

ISSN 2394-3777 (Print)
ISSN 2394-3785 (Online)
Available online at www.ijartet.com
International Journal of Advanced Research Trends in Engineering and Technology (IJARTET)
Vol. 4, Issue 3, March 2017

computed for a local patch about each image pixel. Sharpness maps are constructed at three scales where scale refers to local patch size. By using an integral image [50], sharpness maps may be computed in constant time per pixel for a fixed P and R.

B. Alpha Matting Initialization

Alpha matting is the process of decomposing an image into foreground and background. The image formation model can be expressed as

$$I(x,y) = \alpha_{x,y}F(x,y) + \left(1 - \alpha_{x,y}\right)B(x,y) \quad (3.3)$$

Where the alpha matte, α x,y, is the opacity value on pixel position(x,y). It can be interpreted as the confidence that a pixel is in the foreground. Typically, alpha matting requires a user to interactively mark known foreground and background pixels, initializing those pixels with α =1andα =0, respectively. Interpreting "foreground" as "sharp" and background as "blurred", we initialized the alpha matting process automatically by applying a double threshold to the sharpness maps computed in the previous step to produce an initial value of α for each pixel.

$$mask^s(x,y) = \begin{cases} 1, & if\, m_{LBP}(x,y) > T_{m_1} \\ 0, & if\, m_{LBP}(x,y) < T_{m_1} \\ m_{LBP}(x,y), & otherwise. \end{cases} \quad (3.4)$$

Where s indexes the scale, that is, masks (x,y) is the initial α-map at the s-th scale.

C. Alpha Map Computation

The α-map was solved by minimizing the following cost function as proposed by Levin

$$E(\alpha) = \alpha^T \boldsymbol{L}\alpha + \lambda(\alpha - \hat{\alpha})^T(\alpha - \hat{\alpha}) \quad (3.5)$$

Where α is the vectorized α-map, $\hat{\alpha} = mask^i(x,y)$Is one of the vectorized initialization alpha maps from the previous step, and $\boldsymbol{L}$ is the matting Laplacian matrix. The first term is the regulation term that ensures smoothness, and the second term is the data fitting term that encourages similarity to $\hat{\alpha}$. For more details on Equation 3.5, The final alpha map at each scale is denoted as α s ,s=1,2,3

D. Multi-Scale Inference

After determining the alpha map at three different scales, a multi-scale graphical model was adopted to make the final decision . The total energy on the graphical model is expressed as

$$E(h) = \sum_{s=1}^{3}\sum_{i}\left|h_i^s - \hat{h}_i^s\right| + \beta\left(\sum_{s=1}^{3}\sum_{i}\sum_{j\in N_i^s}\left|h_i^s - h_j^s\right| + \sum_{s=1}^{2}\sum_{i}\left|h_i^s - h_i^{s+1}\right|\right) \quad (3.6)$$

Where $\hat{h}_i^s = \alpha_i^s$ is the alpha map for scale sat pixel location i that was computed in the previous step, and $h_i^s$is the sharpness to be inferred. The first term on the right hand side is the unary term which is the cost of assigning sharpness value $h_i^s$to pixel i in scale s. The second is the pairwise term which enforces smoothness in the same scale and across different scales. The weight β regulates the relative importance of these two terms. Optimization of Equation 3.6 was performed using loopy belief propagation.

ISSN 2394-3777 (Print)
ISSN 2394-3785 (Online)
Available online at www.ijartet.com
International Journal of Advanced Research Trends in Engineering and Technology (IJARTET)
Vol. 4, Issue 3, March 2017

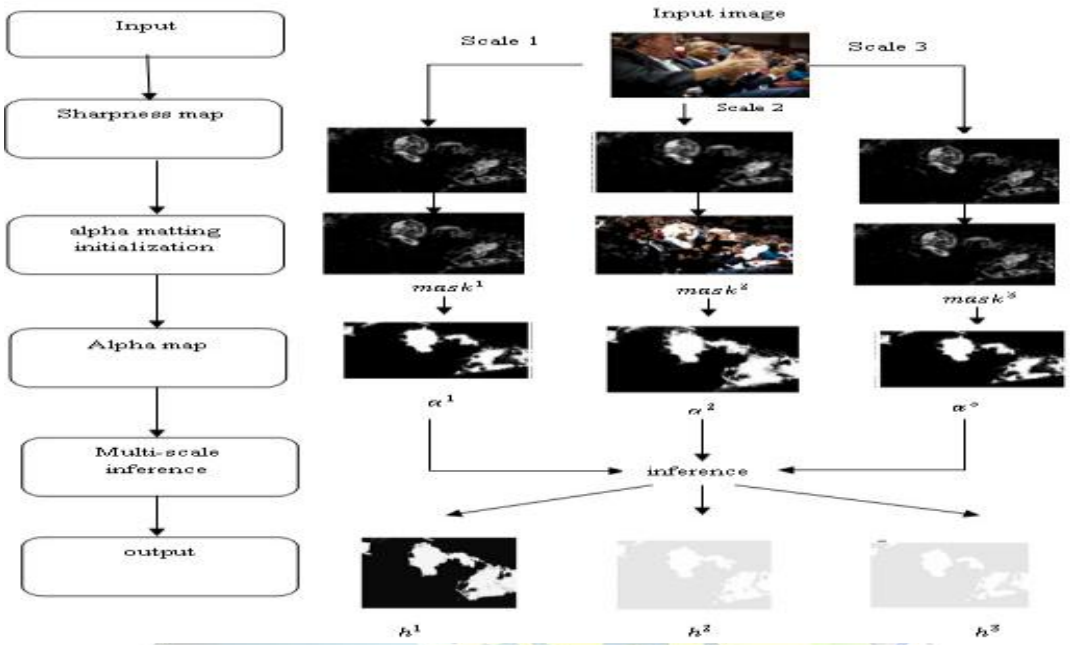

Fig. 3. Our blur segmentation algorithm. The main steps are shown on the left; the right shows each image generated and its role in the algorithm. The output of the algorithm is h 1.

The output of the algorithm is h^3 which is the inferred sharpness map at the largest scale. This is a grayscale image, where higher intensity indicates greater sharpness.

4. SIMULATION RESULTS

```
pre =

    0.8864


rec =

    0.9895

>> tic
>> toc
Elapsed time is 2.760264 seconds.
```

ISSN 2394-3777 (Print)
ISSN 2394-3785 (Online)
Available online at www.ijartet.com
International Journal of Advanced Research Trends in Engineering and Technology (IJARTET)
Vol. 4, Issue 3, March 2017

Figure 4: Result using LBP technique with precision and recall

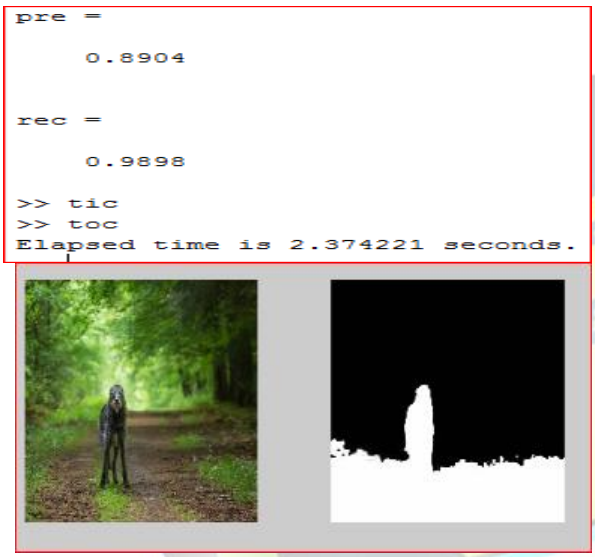

Figure 5: Result using LLBP technique with precision and recall

5. CONCLUSION

We have proposed an exceptionally basic yet compelling sharpness metric for defocus obscure division. This metric depends on the circulation of uniform LLBP designs in obscure and non-obscure picture locales. The immediate utilization of the nearby crude sharpness measure can accomplish similar outcomes to the detail of-the-craftsmanship defocus division technique that in light of meager portrayal, which demonstrates the capability of neighborhood based sharpness measures. By coordinating the metric into a multiscale data proliferation outline work, it can accomplish similar outcomes with the best in class. We have demonstrated that the calculation's execution is kept up when utilizing a naturally and adaptively chose edge Tseg. Our sharpness metric measures the quantity of certain LLBP designs in the nearby neighborhood in this manner can be productively actualized by essential pictures. In the event that joined with continuous tangling calculations, for example, GPU executions of worldwide tangling [18], our technique would have huge speed advantage over alternate defocus division calculations.

REFERENCES

[1] R. Achanta, S. Hemami, F. Estrada, and S. Susstrunk, "Frequency-tuned salient region detection," in Proc. IEEE Conf. Comput. Vis. Pattern Recognit. (CVPR), Jun. 2009, pp. 1597–1604.

[2] H.-M. Adorf, "Towards HST restoration with a space-variant PSF, cosmic rays and other missing data," in Proc. Restoration HST Images Spectra-II, vol. 1. 1994, pp. 72–78.

[3] T. Ahonen, A. Hadid, and M. Pietikäinen, "Face description with local binary patterns: Application to face recognition," IEEE Trans. Pattern Anal. Mach. Intell., vol. 28, no. 12, pp. 2037–2041, Dec. 2006.

[4] S. Bae and F. Durand, "Defocus magnification," Comput. Graph. Forum, vol. 26, no. 3, pp. 571–579, 2007.

[5] K. Bahrami, A. C. Kot, and J. Fan, "A novel approach for partial blur detection and segmentation," in Proc. IEEE Int. Conf. Multimedia Expo (ICME), Jul. 2013, pp. 1–6.

[6] J. Bardsley, S. Jefferies, J. Nagy, and R. Plemmons, "A computational method for the restoration of images with an unknown, spatially-

ISSN 2394-3777 (Print)
ISSN 2394-3785 (Online)
Available online at www.ijartet.com
International Journal of Advanced Research Trends in Engineering and Technology (IJARTET)
Vol. 4, Issue 3, March 2017

varying blur," Opt. Exp., vol. 14, no. 5, pp. 1767–1782, 2006.

[7] A. Buades, B. Coll, and J.-M. Morel, "A non-local algorithm for image denoising," in Proc. IEEE Comput. Soc. Conf. Comput. Vis. Pattern Recognit. (CVPR), vol. 2. Jun. 2005, pp. 60–65.

[8] G. J. Burton and I. R. Moorhead, "Color and spatial structure in natural scenes," Appl. Opt., vol. 26, no. 1, pp. 157–170, 1987.

[9] Christo Ananth, G.Poncelina, M.Poolammal, S.Priyanka, M.Rakshana, Praghash.K., "GSM Based AMR", International Journal of Advanced Research in Biology, Ecology, Science and Technology (IJARBEST), Volume 1,Issue 4,July 2015, pp:26-28.

[10] T. S. Cho, "Motion blur removal from photographs," Ph.D. dissertation, Dept. Elect. Eng. Comput. Sci., Massachusetts Inst. Technol., Cambridge, MA, USA, 2010.

[11] F. Couzinie-Devy, J. Sun, K. Alahari, and J. Ponce, "Learning to estimate and remove non-uniform image blur," in Proc. IEEE Conf. Comput. Vis. Pattern Recognit. (CVPR), Jun. 2013, pp. 1075–1082.

[12] S. Dai and Y. Wu, "Removing partial blur in a single image," in Proc. IEEE Conf. Comput. Vis. Pattern Recognit. (CVPR), Jun. 2009, pp. 2544–2551.